Res Chem Intermed (2013) 39:1003–1014
DOI 10.1007/s11164-012-0611-0

Mesoporous titania photocatalyst: effect of relative humidity and aging on the preparation of mesoporous titania and on its photocatalytic activity performance

Suhaina Mohd Ibrahim · Abdul Kadir Masrom · Babak Mazinani · Shahidan Radiman · Farinaa Md Jamil · Ali Beitollahi · Nobuaki Negishi · Noorhana Yahya

Received: 24 April 2012 / Accepted: 21 May 2012 / Published online: 9 June 2012

Abstract Mesoporous TiO_2 has been synthesized by the sol–gel method, using a nonionic triblock copolymer P123 as surfactant template under acidic conditions. The as-prepared samples were characterized by thermogravimetry–differential thermal analysis (TG–DTA), nitrogen absorption–desorption (BET), field emission scanning electron microscopy, and transmission electron microscopy. The photocatalytic activity of the mesoporous TiO_2 was evaluated by degradation of methylene blue under high-intensity UV light irradiation; the amount of methylene blue was measured by UV–visible spectroscopy. TG–DTA analysis revealed that the surfactant had been removed partly in as-synthesized samples. BET analysis proved that all the samples retained mesoporosity with a narrow pore-size distribution

S. Mohd Ibrahim (✉) · A. K. Masrom · F. Md Jamil
Advanced Material Research Centre (AMREC), SIRIM Berhad, Lot 34, Jalan Hi-Tech 2/3, Kulim Hi-Tech Park, 09000 Kulim, Kedah, Malaysia
e-mail: suenacbw@yahoo.co.uk

B. Mazinani · A. Beitollahi
Department of Metallurgy and Materials Engineering, Iran University of Science and Technology (IUST), Narmak, Tehran, Iran

S. Radiman
School of Applied Physics, Faculty of Science and Technology, Universiti Kebangsaan Malaysia (UKM), Bangi, Selangor, Malaysia

N. Negishi
Institute for Environmental Management Technology, National Institute of Advance Science and Technology (AIST), Tsukuba West, 16-1 Onogawa, Tsukuba 305-8569, Japan

N. Yahya
Faculty of Science and Information Technology, Universiti Teknologi Petronas (UTP), Tronoh, Perak, Malaysia

(4.5–6.3 nm) and high surface area (103–200 m^2/g). All calcined mesoporous TiO_2 had high photocatalytic activity in the photodegradation of methylene blue.

Keywords Mesoporous · TiO_2 · Nonionic triblock copolymer · Photocatalyst

Introduction

Mesoporous non-silica materials have attracted much attention, because they usually have higher surface areas and more uniform and controllable pore sizes and pore morphology than other nanocrystalline materials, and often have unique electronic, magnetic, and catalytic properties [1–6].

However, the synthesis of mesoporous titania with crystalline walls has proved difficult. Transformation from the amorphous phase to the crystalline phase by heat treatment usually induces collapse of the mesopores because the wall is too thin to retain the three dimensional mesoporous structure during crystallization. Strategies to counter this include the use of surfactants during synthesis of mesostructured titania. Peng et al. [7] recently prepared mesoporous anatase TiO_2 nanosized powders with high specific surface areas by using the surfactant cetyltrimethylammonium bromide (CTAB) as a directing and pore-forming agent. In their study it was found that the high photocatalytic activity of the resulting material was related to its large surface area and small anatase crystallites. Sheng et al. [8] prepared nanocrystalline particles at low temperature in the presence of nitric acid by the sol–gel method. The nanocrystalline particles were then used as assembly units to prepare mesoporous TiO_2, using dodecylamine as organic linker. Yu et al. [9] synthesized three-dimensional and thermally stable mesoporous TiO_2, without use of surfactants, by treatment with high-intensity ultrasound irradiation; the high photocatalytic activity of the product was attributed to its high surface area and the three-dimensional connectivity of its mesoporous wormhole frameworks. Many researchers have reported the synthesis of mesoporous titania with uniform mesopores by use of surfactants with ethylene oxide groups of different lengths, and focus on the effects of calcination temperature, aging, pH, porous structure, and pore size on their photocatalytic activity [10–15].

In this paper we report our work on preparation and characterization of mesoporous TiO_2 for enhancing photocatalytic activity by use of a triblock copolymer. In the preparation process we optimized the aging time and relative humidity to ensure that the sample retained its mesoporous structure.

Experimental

Materials

Titanium *n*-butoxide ($Ti(OBu)_4$) was used as titanium precursor. Pluronics triblock copolymer $HO(CH_2CH_2O)_{20}(CH_2CH–(CH_3)O)_{70}(CH_2CH_2O)_{20}H$, designated EO20 PO70EO20 or Pluronic P123 (MW = 5800) was used as the structure-directing

agent, ethanol as a solvent, and acetylacetone (AcAc) as ligand. A mixture of HCl and deionized water was used to control the hydrolysis and condensation reactions of the precursor.

Preparation method chemicals

To prepare mesostructured TiO_2, first, sol A was prepared by dissolving P123 in ethanol with vigorous stirring for 15 min. Second, sol B was prepared by dropwise addition of $Ti(OBu)_4$ to acetylacetone (AcAc) followed by addition of ethanol and stirring of the mixture for 30 min. Sol B was then slowly added dropwise to Sol A and stirred for 2 h; this new solution was known as sol C. Finally, a solution of hydrochloric acid (HCl) in deionized water was added dropwise to sol C and stirring was continued for 3 h at room temperature. The sol C mixture was aged in an oven at 50 °C for 0, 4, 8, or 14 days. The aged sol C solution was transferred to a Petri dish and left in a humidity chamber at 50 or 75 % relative humidity (RH) and 25 °C. After humidification, the sol solution was dried in an oven at 125 °C for one day followed by calcination in a tube furnace for 2 h.

Characterization

Thermogravimetry–differential thermal analysis of mesoporous titania was performed with a SII EXSTAR 6000-TG/DTA6300 from room temperature to 800 °C with a heating rate of 2 °/min under an air flow of 5 mL/min. After degassing of the sample at 150 °C for 6 h, the surface area was measured by use of nitrogen absorption–desorption (BET) with an Autosorb-1 from Quantachrome instruments. Small-angle X-ray scattering (SAXS) measurements were performed with a Kratky compact small-angle system using Kα radiation, and operated at 40 kV and 20 mA, and equipped with a position-sensitive detector containing 1024 channels of width 53.0 mm. The morphology of the samples was characterized by SEM (LEO-1525), with an accelerating voltage of 20 kV, and imaging of the powder was performed with a Philips Tecnai 20 transmission electron microscope (TEM) microscope operated at 200 kV.

Photocatalytic activity

The photocatalytic activity of the TiO_2 mesoporous powder sample was evaluated by measuring the degradation of methylene blue in aqueous solution under high-intensity UV light irradiation. Samples of mass 0.015 g were dispersed in 15 ml 40 or 20 ppm methylene blue to give the ratio of 1 g/L. The TiO_2 powder was dispersed with methylene blue solution in a bottle (in the absence of irradiation) and the bottle was immediately sealed with aluminium foil. For irradiation for 30–150 min, the suspension was placed on a stirrer under high-intensity UV light (mercury lamp 125 W). The concentration spectrum of the TiO_2 powder and the methylene blue was determined by use of UV–Vis spectrometry (at 625 nm wavelength) after centrifugation.

Result and discussion

Thermogravimetric analysis

To obtain mesoporous TiO_2 materials, the block copolymer template must be removed. However, because TiO_2 crystallizes easily, grain growth will certainly occur during the calcination process, it is difficult to remove a template polymer supporting the framework of the TiO_2 mesostructure without causing collapse of the mesostructure [1, 16].

The optimum calcination temperature for all samples was determined by thermal analysis of the TiO_2 gel. As shown in Fig. 1, the sharp peak at 350 °C corresponds to removal of residual organic surfactant. Weight loss stopped at approximately 500 °C, indicating complete removal of organic compounds. On the basis of the literature [1, 17–22], a calcination temperature of 350 °C for 4 h is optimum for calcining mesoporous TiO_2 with complete removal of organic templates and crystallization of the anatase phase, whereas for preparing stable 2D hexagonal mesostructured titania made from a triblock copolymer as the templating agent, a higher calcining temperature of 400 °C for 4 h has been reported. In our experiment, the calcination temperature chosen was 500 °C, because we found this was the most appropriate calcination temperature for preparation of the TiO_2 mesostructure.

N_2 adsorption–desorption analysis

Nitrogen adsorption–desorption isotherms and Barrett–Joyner–Halenda (BJH) pore-size distribution plots of the calcined samples are shown in Fig. 2a–d. All of these

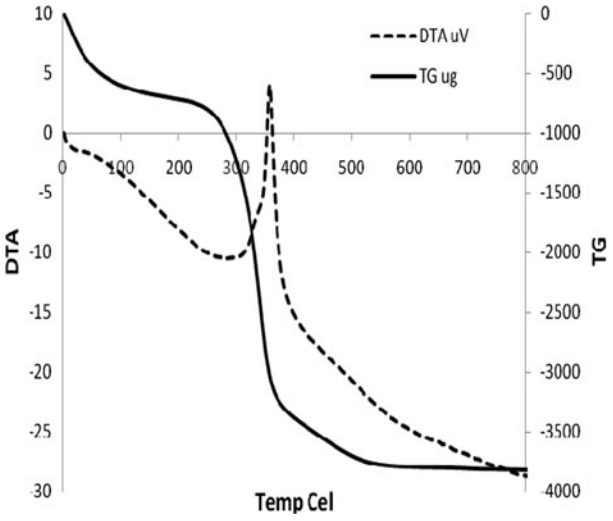

Fig. 1 Thermogravimetric (TG) and differential thermal analysis (DTA) curves for TiO_2 gel

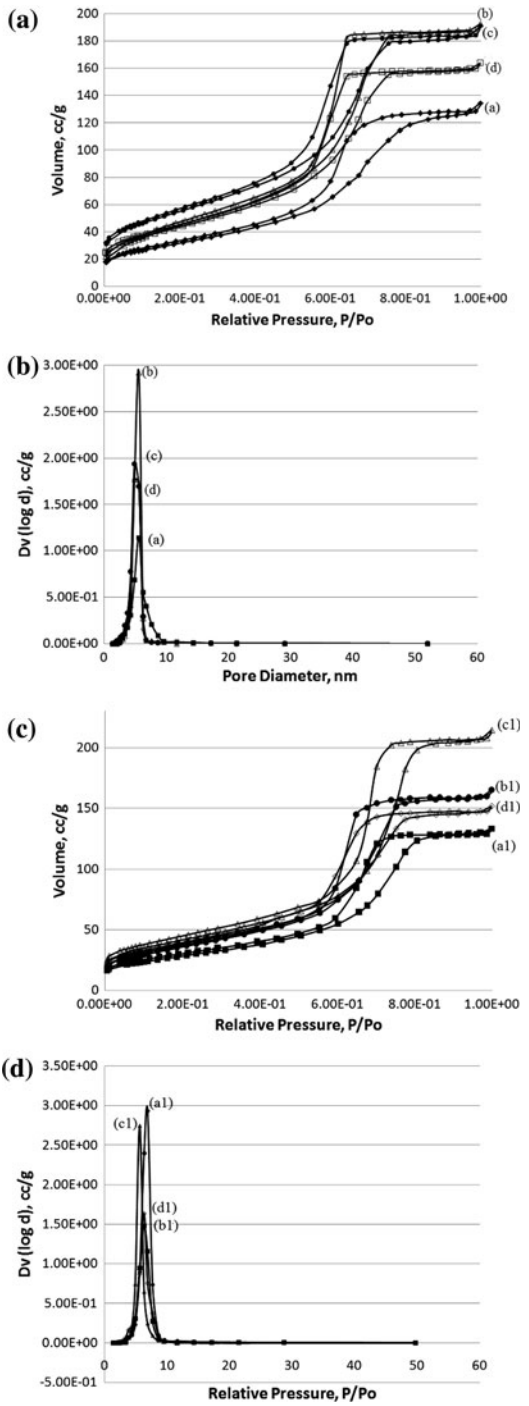

Fig. 2 **a** N_2 adsorption–desorption isotherms for samples aged at RH 50 % for *a* 0, *b* 4, *c* 8, or *d* 14 days. **b** Pore size distribution plots for samples aged at RH 50 % for *a* 0, *b* 4, *c* 8, or *d* 14 days. **c** N_2 adsorption–desorption isotherms for samples aged at RH 75 % for *a1* 0, *b1* 4, *c1* 8, or *d1* 14 days. **d** Pore size distribution plots for samples aged at RH 75 % for *a1* 0, *b1* 4, *c1* 8, or *d1* 14 days

samples had a type IV isotherm with H2 hysteresis loops, which are representative of mesoporous materials.

It is known that H2 hysteresis loops are observed for materials with relatively uniform channel-like pores, when the desorption branch happens to be located at relative a pressure, P/P_o, of approximately 0.4 [8, 20]. The desorption branch of all samples happened to be at a relative pressure, P/P_o, between 0.45 and 0.5, in the region of a lower pressure limit of adsorption/desorption hysteresis for nitrogen adsorption. According to Sing et al. [21] and Yu et al. [22] the hysteresis loop in the pressure range between 0.4 and 0.9 is probably related to the finer intra-aggregated pores formed.

For the samples aged at RH 50 %, it can be seen that the profiles of the adsorption branches on the pressure (x) axes are similar for all the samples except sample a, which means that all these samples have pores of similar shape with narrow openings [23]. For the samples aged at RH 75 %, the adsorption branches for samples a1, b1, and d1 were characteristic of narrow pore openings, and the adsorption–desorption profile also suggested that all samples had uniform pore sizes.

Figures 2a and 3a reveal a strong increase in adsorption values at higher relative pressures for samples b, c, and c1, indicating that aging for 4–8 days leads to higher growth of pore volumes. This could be related to substantial dissolution of the titania skeleton occurring under these aging conditions and creation of interconnectivities between the copolymer and acetylacetone constructing the main pore system. The greater pore volume will also affect the porosity. Using the equations below, the porosity of the samples can be calculated [24].

$$\mathrm{P} = \mathrm{V_p}/\left(\mathrm{V_p} + 0.27\right) \tag{1}$$

$$\mathrm{V_p} = 1.547 \times 10^{-3}\mathrm{V_d} \tag{2}$$

where V_p is the volume of liquid nitrogen corresponding to the total pore volume, which was calculated from the saturation adsorption volume (V_d) at STP. The BET surface areas, pore sizes, pore volumes, and porosities of the samples are summarized in Table 1. The BET results showed that the samples aged at RH 50 % have the highest surface area and porosity but have small pore size compared with samples aged at RH 75 %. This revealed that high humidity could harm the mesoporous structure. This is because the condensation reaction of titanium species probably proceeds before complete evaporation of the solvent. Therefore, the titania aggregates are unable to form a network between the micelles and an ordered mesostructure with large domains could not be formed. It is known that several conditions during aging, including temperature, aging period, and relative humidity, have an important effect on the final mesoporous structure of titania-based systems [5, 25]. The correlation between the values of specific surface area, porosity, and pore size are plotted in Fig. 3.

Small-angle XRD analysis

As shown in Fig. 4a, only one broad peak appeared in the small-angle XRD pattern of sample c; this was attributed to its ordered mesoporous structure (short ordered

Table 1 Summary of surface areas, pore sizes, pore volumes, and porosities of the prepared samples

Sample	Surface area, m^2/g	Pore size, nm	Pore volume, cc/g	Porosity, %
a	116.8	5.62	0.21	43.75
b	171.8	4.70	0.30	52.63
c	199.8	4.51	0.35	56.45
d	161.03	4.84	0.25	48.07
a1	103.2	6.29	0.20	42.55
b1	135.9	5.20	0.23	46.00
c1	151.1	4.90	0.24	47.05
d1	134.8	5.40	0.23	46.00

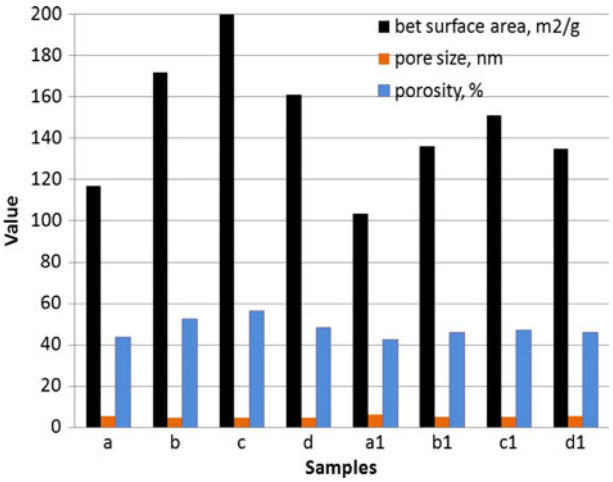

Fig. 3 Correlation between the values of the specific surface area, porosity, and pore size of the prepared samples

structures). This is similar to the pattern for mesoporous silica HMS [26] with a wormhole framework that gave only one broad peak. Moreover, upon thermal treatment at relatively high temperatures, from 500 to 800 °C, the mesoporous structure was gradually destroyed, because of crystallization of the channel walls which destroys the long-range order of the mesoporous structure [15, 27]. We therefore concluded that sample c did not have a layered structure but had a wormhole framework structure. This result was confirmed by TEM observation as shown in Fig. 5b.

Aging conditions can sometimes change the mesostructures from one-dimensional to three-dimensional mesophases for the same system [5]. For both short (1 day) and long (14 days) aging of the titania solution at RH 50 %, Fig. 4a shows small-angle XRD patterns for samples aged at RH 50 % for different times. It can be observed that the broad peak appears only after aging for 4–8 days, corresponding to the formation of large-order domains. This can be explained on

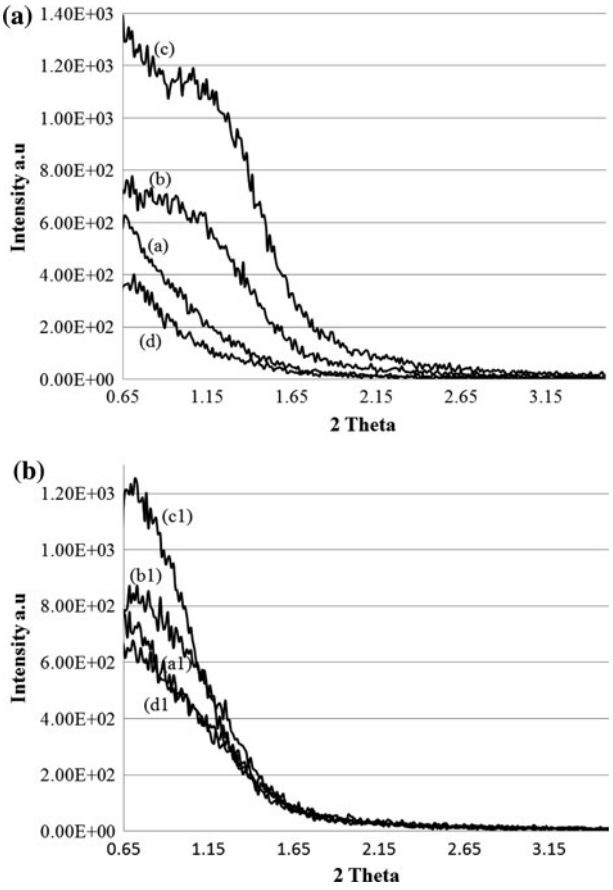

Fig. 4 **a** Small-angle XRD patterns for samples aged at RH 50 % for *a* 0, *b* 4, *c* 8, or *d* 14 days. **b** Small-angle XRD patterns for samples aged at RH 75 % for *a1* 0, *b1* 4, *c1* 8, or *d1* 14 days

the basis that the formation of mesostructured films requires micellar stabilization by gelation of a titania network to constitute the wall structure after the solution has been transferred to The Petri dish. As the solvent gradually evaporates, self assembly of the surfactants starts and their micellization occurs. At the same time, the titania network then stabilizes the micellar organization existing in the solution at the moment of percolation. Therefore, both small fractal unit titania aggregates that are unable to form a percolative network and large units that are unable to occupy the space between micelles cannot form good mesostructured films [13]. It can, therefore, be assumed that other samples that had no peak in small-angle XRD pattern did not have an ordered structure.

It can be seen that when we increased the RH from 50 to 75 % no peaks were observed for the samples (Fig. 4b). This meant relative humidity had a significant effect on mesoporous structure in this study, and confirmed the findings of Oveisi H et al. [5] that lower humidity is a much more suitable aging condition for achieving

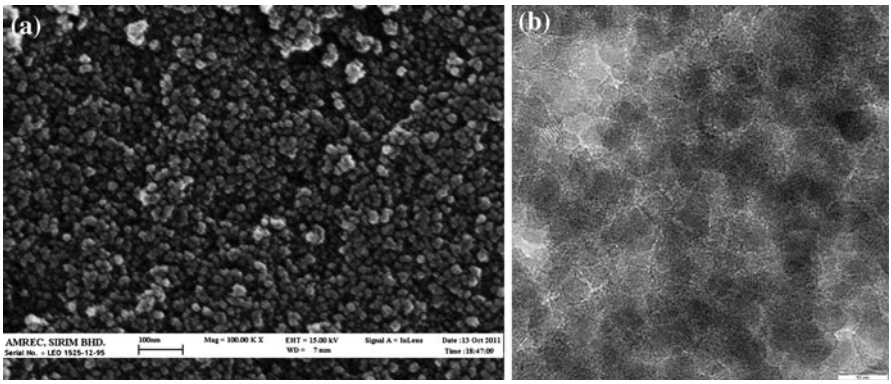

Fig. 5 **a** FESEM **b** HRTEM for sample aged at RH 50 %

greater ordering of the mesostructure [5]. This may be because the condensation reaction of titanium species probably proceeds before complete evaporation of the solvent. Therefore, the titania aggregates are unable to form a network between micelles and ordered mesostructured films with large order domains could not be formed [5, 28–30].

FESEM and HR TEM analysis

Field emission scanning electron microscopy (FESEM) and TEM analysis were conducted to determine the structure of the samples. Figure 5a show the FESEM image of the samples synthesized at RH 50 % aged for 8 days (sample c). To investigate the properties of pores, HR-TEM images were obtained. The HR-TEM image in Fig. 5b clearly shows that particle sizes were irregular, that the pore structure consists of an array of wormhole-like pores, and that the wall of the mesoporous framework consists of interconnected TiO_2 nanoparticles.

Photocatalytic activity

Figure 6a illustrates the progress of photocatalytic degradation of 40 ppm aqueous methylene blue by as-synthesized mesoporous TiO_2 samples. As shown by Fig. 6a all the samples aged at RH 50 % (b,c, and d) degrade the methylene blue more quickly than the sample aged at RH 75 %. The same trend was also shown for degradation of 20 ppm methylene blue (Fig. 6b).

However, it is apparent that the high initial concentration of methylene blue leads to slow degradation, because a constant UV intensity and apparently similar surface area of the prepared sample were used. This phenomenon might be because of the larger quantities of methylene blue molecules absorbed on the surface of the prepared samples leading to the limitation of adsorption of photons from the UV light energy. Consequently, less excitation of the charge carrier by the prepared samples results in slower degradation of (high concentration) methylene blue.

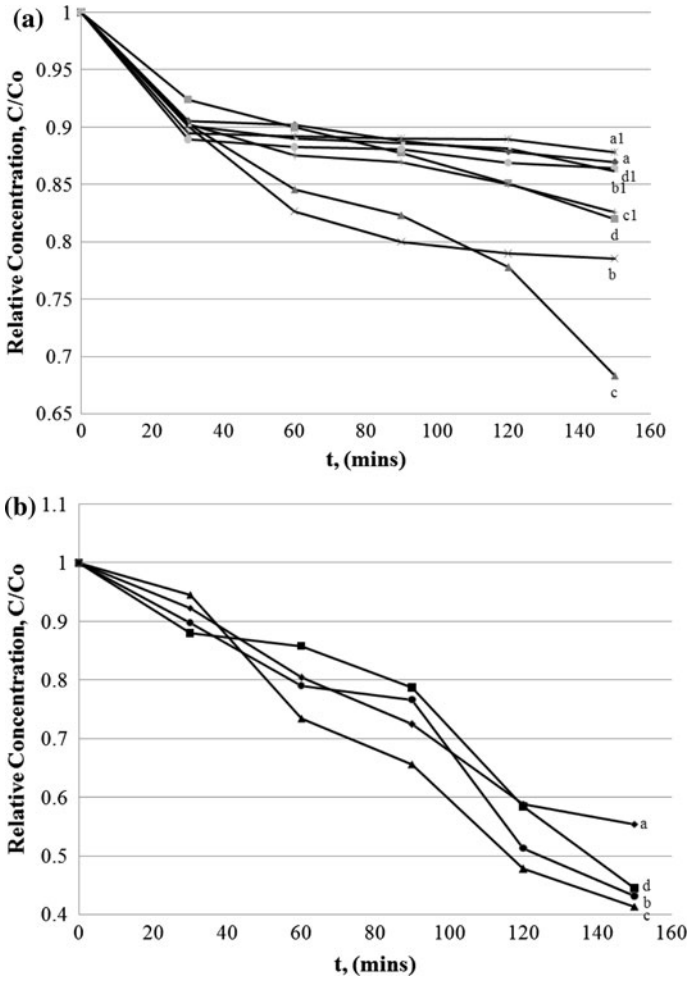

Fig. 6 **a** Changes in the relative concentration of methylene blue (initial concentration 40 ppm) as a function of UV irradiation time for samples aged at RH 50 and 75 %. **b** Changes in the relative concentration of methylene blue (initial concentration 20 ppm) as a function of UV irradiation time for samples aged at RH 50 %

Sample c has the highest photocatalytic activity because of its large surface area (ca. 199.8 m^2/g) and large pore volume (ca. 0.35 cc/g). Large surface area not only efficiently increases the adsorption of reactants, but also enhance light harvesting, capturing more light to generate more electron and hole pairs in the photocatalytic reaction [15, 31]. On the other hand, this sample had a short ordered mesoporous structure compared with other samples, and these pore channels favor transport of the reactant and product molecules [32, 33]. In addition, the wormhole structure of this sample is believed to be one of the important structural features for catalytic activity, because its channel-branching characteristic within the framework provides easy access to reactive sites on the framework wall. This conclusion is in agreement

with research by Kim et al. [34] and Hideaki et al. [35], who stated that silica with wormhole-like framework structures is a more active support than that with a hexagonal structure and comparable uniformity in pore size distributions (e.g., MCM-41, SBA-1 and SBA-15). This therefore proves that photocatalytic activity is highly dependent on surface area and on the structural framework of the sample.

Conclusion

We established that aging time and relative humidity are important in ensuring the sample will have a mesoporous structure. High surface area significantly promotes photocatalytic activity of mesoporous TiO_2. Results showed that the wormhole-like structure of these samples is suitable for degradation of methylene blue because the channel branching within the framework provides easy access to the reactive sites on the framework wall.

Acknowledgments The author acknowledges SIRIM, IUST, UKM, UTP, and AIST for their kind assistance in performing some of the characterization work.

References

1. P.D. Yang, D.Y. Zhao, D.I. Margolese, B.F. Chmelka, G.D. Stucky, Nature **396**, 152 (1998)
2. D.J.A.A. Soler-Illia, A. Louis, C. Sanchez, Chem. Mater. **14**, 750 (2002)
3. Y.K. Hwang, K.C. Lee, Y.U. Kwon, Chem. Commun. 1738 (2001)
4. E. Stathatos, T. Petrova, P. Lianos, Langmuir **17**, 5025 (2001)
5. H. Oveisi, N. Suzuki, Y. Nemoto, P. Srinivasu, A. Beitollahi, Y. Yamauchi, Thin Solid Films **518**, 6714 (2010)
6. J. Rathousky, V. Kalousek, V. Yarovyi, M. Wark, J. Jirkovsky, J. Photochem. Photobiol., A **216**, 126 (2010)
7. T. Peng, D. Zhao, K. Dai, W. Shi, K. Hirao, J. Phys. Chem. B **109**, 4947 (2005)
8. Q. Sheng, S. Yuan, J. Zhang, F. Chen, Microporous Mesoporous Mater. **87**, 177 (2006)
9. J.C. Yu, L. Zhang, J. Yu, New J. Chem. **26**, 416 (2002)
10. D.S. Kim, S.J. Han, S.Y. Kwak, J. Colloid Interface Sci. **316**, 85 (2007)
11. T. Hongo, A. Yamazaki, Microporous Mesoporous Mater. **142**, 316 (2011)
12. H. Yun, K. Miyazawa, I. Honma, H. Zhou, M. Kuwabara, Mater. Sci. Eng., C **23**, 487 (2003)
13. L. Zhao, Y. Yua, L. Songa, M. Ruana, X. Hua, A. Larbot, Appl. Catal. A **263**, 171 (2004)
14. G. Calleja, D.P. Serrano, Rl. Sanz, P. Pizarro, A. Garcıa, Ind. Eng. Chem. Res. **43**, 2485 (2004)
15. G. Li, J.C. Yu, J. Zhu, Y. Cao, Microporous Mesoporous Mater. **106**, 278 (2007)
16. D.M. Antonelli, J.Y. Ying, Angew. Chem. Int. Ed. Engl. **34**, 2014 (1995)
17. D. Grosso, G.J.A.A. Soler-Illia, E.L. Crepaldi, F. Cagnol, C. Sinturel, A. Bourgeois, A. Brunet-Bruneau, H. Amenitsch, P.A. Albouy, C. Sanchez, Chem. Mater. **15**, 4562 (2003)
18. P. Yang, D. Zhao, D.I. Margolese, B.F. Chmelka, G.D. Stucky, Chem. Mater. **11**, 2813 (1999)
19. P.C.A. Alberius, K.L. Frindell, R.C. Hayward, E.J. Kramer, G.D. Stucky, B.F. Chmelka, Chem. Mater. **14**, 3284 (2002)
20. M. Kruk, M. Jaroniec, Chem. Mater. **13**, 3169 (2001)
21. K.S.W. Sing, D.H. Everett, R.A.W. Haul, L. Moscou, R.A. Pierotti, J. Rouquerol, T. Siemieniewska, Pure Appl. Chem. **57**, 603 (1985)
22. X. Yu, S. Liu, J. Yu, Appl. Catal. B:Environ. **104**, 12 (2011)
23. A.D. Marczewska, A.W. Marczewski, I. Skrzypek, S. Pikus, M. Kozak, Appl. Surf Sci. **252**, 625 (2005)

24. B. Yao, L. Zhang, J. Mater. Sci. **34**, 5983 (1999)
25. E.L. Crepaldi, G.J.A.A.S. Illia, D. Grosso, F. Cagnol, F. Ribot, C. Sanchez, J. Am. Chem. Soc. **125**, 9770 (2003)
26. R.P. Thomas, J.P. Thomas, Chem. Mater. **13**, 987 (2001)
27. R.L. Putnam, N. Nakagawa, K.M. McGrath, N. Yao, I.A. Aksay, S.M. Gruner, A. Navrotsky, Chem. Mater. **9**, 2690 (1997)
28. D. Grosso, F. Cangol, G.J.A.A. Soler-Illia, E.L. Crepaldi, H. Amenitsch, A.B. Bruneau, A. Bourgeois, C. Sanchez, Adv. Funct. Mater. **14**, 309 (2004)
29. K.S. Jang, M.G. Song, S.H. Cho, and J.D. Kim, Chem. Commun. 1514 (2004)
30. S.Y. Choi, M. Mamak, N. Coombs, N. Chopra, G.A. Ozin, Adv. Funct. Mater. **14**, 335 (2004)
31. J.C. Yu, X.C. Wang, X.Z. Fu, Chem. Mater. **16**, 1523 (2004)
32. D.R. Rolison, Science **299**, 1698 (2003)
33. H. Wang, J.J. Miao, J.M. Zhu, H.M. Ma, J.J. Zhu, H.Y. Chen, Langmuir **20**, 11738 (2004)
34. S.S. Kim, T.R. Pauly, T.J. Pinnavaia, Chem. Commun. 835 (2000)
35. H. Yoshitake, T. Sugihara, T. Tatsumi, Chem. Mater. 14 (2002)